Published in final edited form as:
*J Mol Cell Cardiol*. 2011 August ; 51(2): 144–155. doi:10.1016/j.yjmcc.2011.04.006.

# Long-term *in vivo* Resistin Overexpression Induces Myocardial Dysfunction and Remodeling in Rats

**Elie R. Chemaly**[*], **Lahouaria Hadri**[*], **Shihong Zhang**, **Maengjo Kim**[¶], **Erik Kohlbrenner**, **Jipo Sheng**, **Lifan Liang**, **Jiqiu Chen**, **Purushothaman K-Raman**, **Roger J. Hajjar**, and **Djamel Lebeche**[#]
Cardiovascular Research Institute, Mount Sinai School of Medicine, New York, NY, USA

## Abstract

We have previously reported that resistin induces hypertrophy and impairs contractility in isolated rat cardiomyocytes. To examine the long-term cardiovascular effects of resistin, we induced *in vivo* overexpression of resistin using adeno-associated virus serotype 9 injected by tail vein in rats and compared to control animals. Ten weeks after viral injection, overexpression of resistin was associated with increased ratio of left ventricular (LV) weight/body weight increased end-systolic LV volume and significant decrease in LV contractility, measured by the end-systolic pressure volume relationship slope in LV pressure volume loops, compared to controls. At the molecular level, mRNA expression of ANF and β-MHC, and protein levels of phospholamban were increased in the resistin group without a change in the level of SERCA2a protein expression. Increased fibrosis by histology, associated with increased mRNA levels of collagen, fibronectin and connective tissue growth factor were observed in the resistin-overexpressing hearts. Resistin overexpression was also associated with increased apoptosis *in vivo*, along with an apoptotic molecular phenotype *in vivo* and *in vitro*. Resistin-overexpressing LV tissue had higher levels of TNF-α receptor 1 and iNOS, and reduced levels of eNOS. Cardiomyocytes overexpressing resistin *in vitro* produced larger amounts of TNFα in the medium, had increased phosphorylation of IκBα and displayed increased intracellular reactive oxygen species (ROS) content with increased expression and activity of ROS-producing NADPH oxidases compared to controls. Long-term resistin overexpression is associated with a complex phenotype of oxidative stress, inflammation, fibrosis, apoptosis and myocardial remodeling and dysfunction in rats. This phenotype recapitulates key features of diabetic cardiomyopathy.

### Keywords

Diabetic cardiomyopathy; cardiac remodeling; resistin; adeno-associated virus 9; hemodynamics; oxidative stress; apoptosis; fibrosis



[#]Corresponding author: Djamel Lebeche, PhD, Cardiovascular Research Institute, AB5-10, Mount Sinai School of Medicine, One Gustave L. Levy Place, Box 1030, New York, NY 10029-6574, Djamel.lebeche@mssm.edu, Tel: 212-241-0322, Fax: 212-241-4080.
[¶]Current address: Mitochondria and Metabolism Center, University of Washington, Box 358057 Seattle, WA 98109-4714
[*]ERC and LH contributed equally to this work.

**Disclosure**
None

## Introduction

Resistin, a novel cysteine-rich hormone secreted by rodent fat cells, had a postulated role in obesity, type 2 diabetes mellitus (T2DM) and insulin resistance [1]. Resistin was shown to be related to inflammation and atherosclerosis [2]. Furthermore, resistin is expressed in cardiomyocytes and was shown to be upregulated by mechanical stretch [3]. Upregulation of resistin in cardiomyocytes by mechanical stretch was found to be mediated by TNF-α [3]. We have recently demonstrated that cardiac tissue from T2DM rats expresses elevated levels of resistin [4]. A variety of cardiovascular effects of resistin were reported since its discovery in 2001; among them are the induction of endothelial dysfunction and the promotion of ischemia-reperfusion myocardial injury [5]. However, the latter finding is controversial with at least one study showing a protective effect of resistin against myocardial ischemia-reperfusion injury [6] and another showing worsening of myocardial ischemia-reperfusion injury by resistin [7]. More recently, resistin blood levels were independently correlated with new onset heart failure in patients [8]. We have shown that adenoviral overexpression of resistin induces hypertrophy in rat neonatal cardiomyocytes, and contractile dysfunction with impaired calcium handling in rat adult cardiomyocytes [9]. The goal of our present study is to determine the long-term cardiovascular effects of resistin overexpression *in vivo* with a cardiotropic adeno-associated virus serotype 9 (AAV9) [10]. The results of this study bring new insights into the mechanisms by which resistin may contribute to cardiac dysfunction in various disease conditions, mainly diabetic cardiomyopathy.

## Methods

### AAV9-Resistin Recombinant Virus Production

293T cells were co-transfected with pTR-Resistin and pDG-9 (expressing AAV9 capsid and helper functions) under the control of CMV promoter by calcium phosphate method. Three days after transfection cells were harvested, washed in 1X PBS, and resuspended in 150 mM NaCl, 50 mM Tris. Virus was released by 3 cycles of freeze/thaw, and Benzonase and $MgCl_2$ were added to a final concentration of 150 units/ml and 2 μM respectively. The cell lysate was incubated for 30 minutes at 37°C then centrifuged at 3400 g for 20 minutes. The supernatant was loaded onto an iodixanol gradient and centrifuged for 1 hour at 69,000 rpm at 18°C. The virus was extracted from the 40%–60% interface and the bottom portion of the 40% fraction. The iodixanol fractions containing virus were concentrated and at the same time buffer was exchanged to Lactated Ringer's solution, then filtered with a 0.2 μm syringe driven filter. Stocks were stored at −80°C, and genome-containing particles were determined by qPCR.

### Animals and virus injection

Animals were handled as approved by local Institutional Animal Care and Use Committees in accordance with the "Principles of Laboratory Animal Care by the National Society for Medical research and the Guide for the Care and Use of Laboratory Animals" (NIH Publication No. 86–23, revised 1996).

200–250 grams male Sprague-Dawley rats were injected with AAV9 overexpressing resistin (AAV9-Retn) (n=5) or control (n=8). Animals received $4\times10^{11}$ drp (DNase resistant particles) in the tail vein under sedation by isoflurane inhaled through wet gauze in an aspiration hood. The vector and its dose were chosen based on the established cardiotropism of AAV9, and on the amount of virus and duration of infection we showed in previous studies to transduce a significant fraction of cardiomyocytes [10].

## Echocardiography

Echocardiographic data were obtained at baseline (before virus injection, or at a similar age and weight for control animals) and at 10 weeks post injection. Echocardiography was performed under sedation with ketamine 80–100mg/kg injected intraperitoneally. Sedation was optimized by (1) giving the lowest dose of ketamine needed to restrain the animal and prevent motion artifact (2) maintain the heart rate as close as possible to 400 beats/minute. Short-axis parasternal two dimensional (2D) views of the left ventricle (LV) at the mid-papillary level and long-axis parasternal views of the LV were obtained using a Vivid7 echocardiography apparatus with a 14MHz linear array probe (i13L probe, General Electric, New York, NY). M-mode measurements of the size of the LV walls and cavities were obtained by 2D guidance from the short-axis view of the LV as recommended by the American Society of Echocardiography [11]. Volumes of the LV cavity in end-systole and end-diastole were calculated using an area-length formula where the LV is assumed to be bullet-shaped as previously recommended and described [11, 12]. LV end-diastolic and end-systolic volumes (respectively EDV and ESV) were thus calculated as follows:

$V=\frac{5}{6}\times A\times L$ where V is the volume of the LV cavity in ml, A is the cross-sectional area of the LV cavity in $cm^2$ obtained from a parasternal short axis image at the mid-papillary level, and L is the length of the LV cavity measured as the distance from the endocardial LV apex to the mitral-aortic junction on the parasternal long-axis image as previously described [12].

## Invasive hemodynamics by pressure-volume loop analysis of the LV

At end-point, LV pressure-volume (P-V) loops were obtained as previously described [13]. Briefly, rats were anesthetized with inhaled 5% (volume/volume) isoflurane for induction, and subsequently intubated and mechanically ventilated. Isoflurane was lowered to 2 – 3% (volume/volume) for surgical incisions. The chest was opened through a median sternotomy. A 1.9F rat P-V catheter (Scisense, London, Ontario, Canada) was inserted into the LV apex through an apical stab performed with a 25GA needle. Hemodynamic recordings were performed after 5 minutes of stable heart rate. Anesthesia was maintained at 0.5–1% isoflurane to keep the animal sedated and maintain a stable heart rate around 350 beats/minute. Hemodynamics were recorded subsequently through a Scisense P-V Control Unit (FV8968). The intrathoracic inferior vena cava was transiently occluded to vary venous return during the recording to obtain load-independent P-V relationships. Linear fits were obtained for end-systolic pressure volume relationships (ESPVR) and end-diastolic pressure-volume relationships (EDPVR). We slowly injected 50μl of 30% NaCl into the external jugular vein for ventricular parallel conductance (Vp) measurement as previously described [13]. Volume measurements were calibrated using blood-filled cuvette of known volumes, and pressure sensors were calibrated as per manufacturer's instructions.

## Animal sacrifice and tissue harvesting

Upon termination of the invasive hemodynamics measurements, animals were sacrificed; LV and right ventricular tissues were separated and weighed. A ring of LV tissue was embedded for histological studies and the rest of the LV tissue was frozen for RNA and protein analysis.

## Blood glucose measurement

Capillary blood glucose was measured from resistin-overexpressing and age and weight-matched control animals under ketamine sedation, shown not to affect blood glucose [14], using a commercial glucometer.

### Protein quantification by western blot analysis

Protein samples were prepared from either isolated cardiomyocytes or rat LV tissue using a lysis buffer containing protease inhibitors (Roche). Protein lysates were matched for protein concentration and then separated by SDS-PAGE and transferred onto polyvinlylidene difluoride membranes (Bio-Rad). The membranes were blocked in 5% nonfat milk and incubated overnight at 4°C with antibodies against resistin (Biovision), $Bcl_2$, Bax, Nox2, Nox4, $p22^{phox}$, $p47^{phox}$ and nitrotyrosine (Santa Cruz Biotechnology), GAPDH (Sigma), iNOS and eNOS (BD Transduction Laboratories), phospholamban (PLB) (Badrilla) and SERCA2a (custom made in our laboratory). The membranes were incubated with appropriate secondary antibodies and signal intensities were visualized by enhanced Chemiluminescence (Pierce) or the Odyssey 2-color detection system. Films from at least three independent experiments were scanned and densities of the immunoreactive bands were evaluated using NIH Image software. Protein loadings were verified against GAPDH densities.

### RNA quantification by quantitative real time PCR

RNA was obtained from LV tissue or cardiomyocytes in culture using standard procedures. Expression was quantified for the following genes: atrial natriuretic factor (ANF), beta myosin heavy chain (β-MHC), connective tissue growth factor (CTGF), fibronectin, collagen subtypes (COL3A1, COL1A2, COL1A1), TNF-α receptor 1, actin and 18S rRNA. Quantification was performed using the ABI-7500 real-time PCR system (Applied Biosystems) and rat specific primers. For each set of primers, a no template control and a no reverse transcription control were included. Post-amplification dissociation curves were performed to verify the presence of a single amplification product in the absence of genomic DNA contamination. Fold changes in gene expression were determined using the ΔΔCt method with normalization to endogenous controls.

### Histological assessments of fibrosis, apoptosis and Intracellular Superoxide

**Assessment of fibrosis—**Serial 8 μm frozen sections from LV tissue were stained with Sirius Red or Masson trichrome following the manufacturer's instructions. Cardiac fibrosis was quantified on Masson trichrome-stained sections with image pro Plus Software. Sirius red stained slides from resistin-overexpressing and control LV were used to quantify the areas of collagen I and III (Total collagen area). Using an Olympus microscope BX50 in 20x magnification field, slides were measured under polarization microscopy using the polarizer objective and filter. Color intensities for collagen I (red polarized area) and Collagen III (green polarized area) were manually traced and planimetered using the different color intensity grade and calibrated with the Zedec (Quantum Inc.) software, adopting a pre-determined calibration scale in mm for 20x objective. Collagen I and III (Total collagen area) were quantified in the entire cross-sectional area of ventricular myocardium in resistin and control animals.

**Assessment of apoptosis—**Serial 8 μm frozen sections from LV tissue were fixed in 1% paraformaldehyde for 10 minutes at room temperature and post-fixed in Ethanol/Acetic acid (2:1) for 5 minutes at 20°C. Detection of apoptotic cells was achieved by direct immunofluorescence detection using terminal deoxynucleotidyl transferase (TdT)-mediated dUTP nick end labeling (TUNEL) (ApopTag detection kit, Millipore). Tissue sections were then counter-stained with DAPI stain (Victor), and viewed with a micro-optics microscope (Carl Zeiss) equipped with filter sets for rhodamine and DAPI staining. To quantify apoptosis, six to seven randomly selected microscopic fields per section zone of each ventricular sample were examined. The percentage of apoptotic cells was determined by

counting the total number of nuclei and TUNEL positive nuclei (apoptotic cells). Sections of interest were photographed using a microscope-integrated 35-mm camera.

**Assessment of intracellular Superoxide content—**Production of superoxide was determined in serial 8 μm frozen sections from LV tissue using dihydroethidium (DHE) staining. Tissue sections were incubated with 10 μmol/L DHE at 37°C for 30 min in a light-protected humidified chamber. Ethidium fluorescence (excitation at 490 nm, emission at 610 nm) was examined by fluorescence microscopy.

### Isolation and Culture of rat adult Cardiomyocytes and infection with adenovirus for in vitro studies

Ventricular cardiomyocytes were prepared and infected with adenovirus expressing resistin or a corresponding control virus as we described previously [9].

### Assessment of TNF-α released by cardiomyocytes in culture

Twenty four hours after cardiomyocyte infection with adenovirus encoding for resistin or β-gal (control), supernatants were collected and assayed for TNFα content using an ELISA assay kit specific for rat TNFα according to manufacturer's instructions (Pierce). Results of 3 independent experiments were expressed as percentage of β-gal as control and defined as 100%.

### NADPH oxidase activity

The activity of NADPH oxidase was determined in adult rat cardiomyocytes using a lucigenin-enhanced chemiluminescence assay. Adult rat cardiomyocytes were infected with adenovirus encoding for resistin or β-gal and cultured for 48 hours before harvesting. The reaction was started by the addition of a mixture of 5 μmol/L lucigenin and 0.1 mM NADPH to 25 μg of protein samples in a final volume of 300 μl in the absence or presence of 300 nmol/L apocynin (an inhibitor of NADPH oxidase activity). The chemiluminescence was continuously recorded using a luminometer. A buffer blank was subtracted from each reading.

### Statistical analysis

Data were expressed as mean ± SD. Comparisons of quantitative variables between groups used a Student's *t* test. $P<0.05$ was considered statistically significant.

## Results

### Glucose levels following resistin overexpression

Certain studies have reported physiological roles of resistin in glucose regulation in liver, and adipose tissues. We therefore measured serum glucose levels and observed that resistin-overexpressing (AAV9-Retn) animals showed significant but modest hyperglycemia compared to controls (8.47 ± 1.54 vs. 6.66 ± 0.83 mmol/L, $p<0.05$), suggesting that resistin may interfere with glucose metabolism *in vivo*. However, in other studies, the glucose level was not affected by overexpressing resistin in mice using intravenous administration of recombinant adenovirus encoding mouse resistin gene [15, 16].

### Echocardiographic and morphometric analysis of the left ventricle

As a first assessment of the effect of resistin on cardiac function we utilized non-invasive transthoracic echocardiography in resistin-transduced and control animals. Left ventricular function and dimensions were measured at baseline and 10 weeks post-viral injection. Echocardiographic and cardiac morphometric analyses of control or resistin-overexpressing

rats left ventricles (LV) at 10 weeks are shown in Table 1. Baseline echocardiographic data did not differ between the two groups (data not shown). Compared to controls, resistin-overexpressing rats had an increased ratio of LV weight/body weight (1.64±0.10 vs. 1.88±0.13 mg/g, $p$ <0.05) and an increase in the end-diastolic diameter (6.6±0.3 vs. 7.1±0.5mm, $p$ <0.05) and end-systolic volume (0.06±0.02 vs. 0.10±0.03 ml, $p$ <0.05).

### Left Ventricular invasive hemodynamics

To further elucidate the effect of resistin on cardiac function *in vivo*, we conducted a left ventricular pressure-volume (PV) analysis. A representative PV loop tracing during vena cava occlusion is shown in Fig. 1A. PV analysis revealed abnormalities in LV contractility; the slope of the end-systolic pressure volume relationships (ESPVR) was significantly reduced in resistin animals (0.86±0.24 mmHg/μl vs. 0.37±0.08 mmHg/μl; $p$<0.01) (Fig. 1A; Table 2). Based on the linear fitting (slope and intercept) of the ESPVR, pressures at 0, 100, 150 and 200 μl of end-systolic volumes were calculated and were significantly lower in the resistin group starting at 150μl of volume (Fig. 1B).

### Resistin expression is increased in LV tissue of AAV9-Retn injected animals

We next examined the expression level of resistin in AAV9-Retn hearts. Quantitative real time RT-PCR and western blot analyses demonstrated significantly higher mRNA (4.39-fold; $p$<0.001) (Fig. 2A) and protein (1.5-fold; $p$<0.001) (Fig. 2B) expression levels of resistin in LV tissue of AAV9-Retn injected animals compared to control animals. In addition, we observed that dimeric resistin (MW ~25kDa; Fig. 2B) is mostly expressed following AAV9-Retn transduction *in vivo*.

Although AAV9 has been postulated to have increased cardiac tropism and robust myocardial expression, it still can infect liver and renal tissues. We therefore evaluated resistin expression in the liver and the kidney following AAV9-Retn transduction. Western blot analysis demonstrated that the level of resistin protein, in the liver and the kidney, is identical in control and AAV9-Retn groups (Fig. 2C), indicating that the cardiac overexpression of resistin did not alter the level of endogenous resistin in these tissues.

### Effect of resistin overexpression on molecular markers of cardiac hypertrophy and calcium handling proteins

As reported earlier, the resistin group has an increased LVW/BW ratio, an indication of cardiac hypertrophy. To further characterize the hypertrophic response following the long-term overexpression of resistin we examined, by quantitative real time RT-PCR, the expression of two molecular markers of stress and hypertrophy, atrial natriuretic factor (ANF) and β-myosin heavy chain (β-MHC). As shown in figures 3A and 3B, respectively, resistin induced a significant increase in ANF (1.92-fold; p<0.05) and β-MHC (1.40-fold; p<0.05) mRNA levels in LV tissue of AAV9-Retn-injected animals compared to controls.

In *vivo* hemodynamics analysis showed impaired contractility following resistin overexpression (Fig. 1B). Since the sarcoplasmic reticulum calcium cycling affects cardiac function and depends largely on the SERCA2a/PLB ratio [17], a good indicator of cardiac contractility, we investigated the effect of resistin overexpression on SERCA2a and phospholamban (PLB) protein levels by western blot (Fig. 3C). We observed no change in the protein level of SERCA2a (Fig. 3E) but a significant increase in the expression of the endogenous SERCA2a inhibitor, phospholamban (Fig. 3D), leading to a decreased SERCA2a/PLB ratio. These findings are consistent with our *in vitro* data [9] and may partially explain the observed impairment in cardiac contractility by resistin.

### Resistin overexpression increases oxidative stress

It is widely recognized that reactive oxygen species (ROS) are associated with several cardiovascular diseases, such as hypertension, cardiac hypertrophy and heart failure [18, 19]. Recent evidence indicates that NADPH oxidase is a major myocardial ROS source [18, 20], whose activity and subunits expression are increased in experimental models of LV hypertrophy and heart failure [18, 20–22]. Since the role of resistin in the production and the activation mechanisms of myocardial ROS has not been studied before, we wanted to examine the degree of resistin involvement in this process. We first determined the intracellular ROS content in frozen ventricular tissue sections from AAV9-Retn and control rats. Dihydroethidium fluorescence staining, a relatively specific marker of superoxide, is significantly stronger in AAV9-Retn hearts compared to controls (Fig. 4A), indicating increased ROS production. We then determined whether the increase in ROS production is attributable to the activation of NADPH oxidase, a superoxide-producing enzyme, in adult rat cardiomyocytes, either non-infected (Cont) or infected with adenovirus encoding for resistin or β-gal in the absence or presence of apocynin (an inhibitor of NADPH oxidase activity). The superoxide producing activity of NADPH oxidase was measured by lucigenin chemiluminescence. Resistin overexpression significantly increased NADPH oxidase activity compared to β-gal (48.78 ± 1.94 arbitrary units (AU)/μg protein vs. 24.29 ± 0.84; $p<0.001$); however, the resistin-induced increase in NADPH oxidase activity was remarkably blunted by apocynin (24.08 ± 1.83 AU; $p<0.001$) (Fig. 4B), suggesting NADPH oxidase as a likely major source of myocardial superoxide induced by resistin. To further elucidate the mechanisms underlying resistin-induced NADPH oxidase activation in cardiomyocytes, we analyzed the expression of key NADPH oxidase isoforms and associated subunits, Nox2 and Nox4, $p47^{phox}$ and $p22^{phox}$. We also analyzed the expression of nitrotyrosine, which also an important molecular indicator of ROS. Immunoblotting analyses showed that cardiomyocytes overexpressing resistin expressed significantly higher levels of Nox2 (2.11 ± 0.06 AU vs. 1.08 ± 0.04; *p<0.001*), Nox4 (0.83 ± 0.06 AU vs. 0.38 ± 0.07; *p<0.01*), $p47^{phox}$ (0.44 ± 0.06 AU vs. 0.21 ± 0.03; *p<0.01*) and nitrotyrosine (2.80 ± 0.26 AU vs. 1.45 ± 0.54; *p<0.01*) compared to β-gal-transduced cells (Fig. 4C). Resistin also induced a considerable elevation in $p22^{phox}$ expression (1.28 ± 0.13 AU vs. 0.73 ± 0.16; *p=0.058*) (Fig. 4C). These results demonstrate that the resistin-induced enhancement of NADPH oxidase activity correlates with increased expression of NADPH oxidase and ROS-associated proteins. Altogether, these data suggest that resistin plays a critical role in mediating NADPH oxidase-derived ROS production in the heart and establish it as a proinflammatory mediator in the myocardium.

### Resistin overexpression increases proinflammatory proteins in LV tissue and in isolated adult cardiomyocytes

Excessive ROS production can trigger inflammatory responses and provoke the up-regulation of inflammatory cytokines. In addition, recent studies reported that resistin can trigger a proinflammatory state in adipose tissues and in human and mouse macrophages [23–25]. Since we showed that resistin stimulates ROS generation, we sought to evaluate resistin's action on inflammatory cytokines in the myocardium. Resistin over-expressing LV tissue had an increase in the mRNA level of TNF-α-receptor 1 (Fig. 5A), while adult cardiomyocytes infected with adenovirus overexpressing resistin (Ad.Retn) released larger amounts of TNF-α in the medium compared to control myocytes (Fig. 5B) and displayed increased phosphorylation of IκB-α (Fig. 5C and D). The activation of the transcription factor NFκB is an essential step in cytokines-induced inflammation, and the phosphorylation and degradation of IκB-α protein is pre-requisite for NFκB activation. The observation that resistin overexpression stimulates TNF-α production and IκB-α phosphorylation supports a myocardial pro-inflammatory effect of resistin *in vivo*.

### Resistin overexpression increases fibrosis in LV tissue

Myocardial fibrosis is a hallmark of cardiac hypertrophy and heart failure. Recent evidence demonstrated that induced ROS is associated with increased extracellular matrix turnover and control of fibroblasts differentiation [26, 27]. We therefore wanted to explore whether resistin plays a role in the regulation of myocardial fibrosis following its overexpression. Indeed, histological analysis showed large amounts of fibrosis in AAV-9-Retn-treated animals as demonstrated by Sirius red or Masson Trichrome staining (Fig. 6A) compared to controls. Quantitative analyses of collagen content (Fig. 6B) and fibrosis (Fig. 6C), were significantly increased following resistin overexpression in LV tissues. To elucidate the molecular mechanisms of resistin-induced fibrosis, we determined the expression levels of key profibrotic targets. mRNA analysis revealed that resistin overexpression increased mRNA expression levels of collagen 1 and 3 subtypes (Fig. 6D), connective tissue growth factor (CTGF) (1.88-fold, $p<0.05$; Fig. 6E), and fibronectin (1.51-fold, $p<0.05$; Fig. 6F). These data clearly demonstrate that resistin upregulation is associated with increased myocardial fibrosis *in vivo*.

### Resistin increases apoptosis in LV tissue and in vitro in adult cardiomyocytes

The increase in cardiac fibrosis induced by resistin prompted us to examine the degree of apoptosis in AAV9-Retn hearts. Using the Tunnel assay on LV tissue sections, we found a significant increase in the number of apoptotic cells in animals injected with AAV9-Retn compared to control animals (0.2 ± 0.05% vs. 0.025 ± 0.001%; $p<0.05$) (Fig. 7A). To elucidate the mechanisms underlying the pro-apoptotic effect of resistin, we assessed the expression levels of key proteins involved in the apoptotic cascade. LV tissue from resistin-injected animals expressed lower protein levels of Bcl-2 (anti-apoptotic) and a remarkable trend of higher levels of Bax (pro-apoptotic) (Fig. 7B, $p=0.05$). In cultured adult rat cardiomyocytes infected with an adenovirus expressing resistin, we noted a similar pro-apoptotic pattern compared to those infected with adenovirus expressing β-galactosidase with increased Bax expression and decreased Bcl-2 expression (Fig. 7C). In addition, an increase in the protein levels of cleaved caspase-3, an active element involved in the apoptotic pathway, was also noted in cardiomyocytes overexpressing resistin (Fig. 7D). Altogether, these observations suggest that resistin may induce a lower Bcl-2/Bax ratio that promotes the release of mitochondrial apoptotic signals and stimulates cell death.

### Resistin differentially modulates iNOS and eNOS expression in the myocardium and in cardiomyocytes

Since iNOS is a target of TNF-α/NFκB signaling and can activate Bax expression leading to apoptosis, we assessed its expression in LV tissues following resistin overexpression. The expression of the protein iNOS was significantly up-regulated in LV tissue from animals injected with AAV9-Retn compared to controls (1.2 ± 0.13 AU vs. 0.84 ± 0.02 AU; $p<0.05$) (Fig. 8A). There was a trend to a decreased expression of eNOS in resistin-overexpressing LV tissue (1.64 ± 0.37 AU vs. 3.26 ± 0.75 AU; $p=0.06$) (Fig. 8A). Moreover, isolated adult cardiomyocytes overexpressing resistin had higher protein levels of iNOS (1.95 ± 0.02 AU vs. 1.32 ± 0.03 AU; $p<0.05$) (Fig. 8B) and lower protein levels of eNOS (0.19 ± 0.02 AU vs. 0.38 ± 0.04 AU; $p<0.05$) (Fig. 8C) compared to myocytes overexpressing β-galactosidase.

## Discussion

Resistin, an adipokine, is thought to play an important role in insulin resistance, diabetes, obesity, and cardiovascular disease, in humans and in rodents [1, 2, 5, 8]. Clinical studies have indicated that increased circulating concentrations of resistin were associated with incident heart failure, even after accounting for prevalent coronary heart disease, obesity, and measures of insulin resistance and inflammation [8], suggesting a distinct cardiac impact

of this protein. In this study, we present evidence that long-term overexpression of resistin by AAV9 vector in rat hearts was associated with features of cardiac remodeling and hypertrophy, myocardial dysfunction, and alterations in myocardial calcium handling. We further show *in vivo* and *in vitro* evidence of ROS activation, myocardial inflammation, fibrosis and apoptosis with an increase in iNOS and a decrease in eNOS; the dynamic changes in the expression of iNOS and eNOS were, interestingly, also manifested in isolated cardiomyocytes overexpressing resistin. In a previous study, we had shown that short-term overexpression of resistin in adult and neonatal rat cardiomyocytes altered cellular contractility and intracellular calcium handling, and promoted cardiomyocyte hypertrophy [9]. Our multiple findings on the consequences of long-term resistin overexpression recapitulate the major characteristics of diabetic cardiomyopathy and suggest that resistin may be a molecular determinant of diabetic cardiomyopathy. Diabetic cardiomyopathy is now recognized as multifactorial disease which involves a variable combination of left ventricular hypertrophy, myocardial lipotoxicity, increased oxidative stress, myocardial diastolic and systolic dysfunction, impaired myocardial calcium handling; myocardial fibrosis, apoptosis and inflammation [28, 29].

We observed a mild increase in the ratio of LV weight/body weight, and an increase in the expression of the hypertrophic markers ANF and β-MHC, along with an increase in the expression of the recently identified prohypertrophic CTGF [30, 31]. It is not possible, given our data, to rigorously conclude that this constellation of molecular findings represents a hypertrophic phenotype or the result of inflammation and stress. It has been shown that TNF-α can by itself upregulate β-MHC [32] through a switch of cardiomyocyte transcriptional profile. Besides, in a study showing a worsening of myocardial ischemia-reperfusion injury by resistin, the effect was acute, mediated by IκB phosphorylation, and associated with an increased secretion of the atrial natriuretic peptide [7]. The cross-talk between TNF-α, NFκB and resistin was shown in previous studies, where TNF-α mediates the upregulation of resistin in response to mechanical stretch of cardiomyocytes [3]; conversely, resistin infusion was shown to induce TNF-α production in isolated perfused hearts and worsen ischemia-reperfusion injury by a mechanism dependent on IκB phosphorylation [7]. In terms of the prohypertrophic effect of CTGF and its impact on cardiac function, these phenomena were mild and delayed in transgenic animals overexpressing CTGF [31], although in isolated cardiomyocytes, it directly induced hypertrophy [33]. CGTF is widely expressed and is particularly implicated in fibrosis. Expression of CGTF is up-regulated by TGF-β in cardiac fibroblasts and myocytes, and also in rodent hearts in experimental models of hypertension, diabetes, and myocardial infarction, and in human ischemic hearts. It is therefore probable that CGTF is involved in fibrosis in pathological situations. We have previously shown that CGTF enhances pressure overload-induced cardiac fibrosis [33]. Upregulation of CGTF expression in PE and ET-1-treated neonatal cardiomyocytes also suggested that CGTF may propagate hypertrophic responses of cardiomyocytes subsequent to initial stimuli, and may also contribute to the increase in fibrosis which occurs in cardiac hypertrophy. In addition, previous studies have demonstrated the direct role of TNF-α in myocardial fibrosis induced by diabetes [34], however, fibrosis and apoptosis (another feature of cardiac remodeling observed in this study as a result of resistin overexpression) in long-term diabetes were reported after shorter term inflammation had subsided [35]. TGF-β1, through CTGF, is thought to mediate fibrosis and apoptosis in the latter study [35]. Increased fibrosis in resistin-transduced hearts, which coincided with increased expression of fibrotic markers – collagen, CGTF, fibronectin – clearly establishes resistin as a profibrotic mediator although the mechanisms by which resistin promotes the development of a fibrogenic cardiac phenotype are yet to be determined.

Our findings on myocardial dysfunction related to resistin can be explained, at least in part, by the upregulation of TNF-α and ANF, both thought to exert negative inotropic effects [7] and, in the case of TNF-α, impair calcium handling. We also demonstrate a unique pattern of increased expression of phospholamban with unchanged expression of SERCA2a. Increased levels of total phospholamban were previously demonstrated in diabetic rat hearts [36]. This observation is interesting since it suggests that resistin may elicit its effects on signaling transduction by other mechanisms including calcium-dependent cascades. In particular, phospholamban has been reported to be implicated in cardiomyocyte apoptosis through a calcium-dependent pathway [37, 38]. We have also previously shown that resistin alters intracellular calcium handling and increases diastolic calcium [9]. Since changes in calcium cycling play a key role in cellular apoptosis [39], it is interesting to note that, at least part, the detrimental effects of resistin may be attributed to its ability to dysregulate calcium homeostasis in cardiomyocytes. Our data also support a direct role of resistin in the regulation of myocardial cell apoptosis. We observed for the first time that chronic cardiac-specific overexpression of resistin induced cardiac cell death. The underlying mechanisms may involve altered expression of anti- and pro-apoptotic molecules, Bcl-2 and Bax, respectively. Apoptosis has recently been recognized as an important factor in heart failure development [40]. Thus, increased apoptosis may contribute to the observed cardiac dysfunction following long-term resistin expression.

*In vivo* resistin overexpression resulted in an increased expression of iNOS and a decreased expression of eNOS. Although it has been shown that resistin can induce endothelial dysfunction [41, 42], our *in vitro* data indicate that iNOS and eNOS in isolated cardiomyocytes have their expression modulated by resistin. This pattern of expression change in myocardial iNOS and eNOS can be at the same time a cause and a consequence of adverse cardiac remodeling, and iNOS was shown to be upregulated by TNF-α [43]. However, considering the controversies in the role and dynamic change of myocardial iNOS and eNOS in pathologic conditions [43], their connection with resistin may need further studies.

An important aspect that our study demonstrates is the ability of resistin to stimulate the production of ROS. This is documented by the remarkable elevation in intracellular superoxide content and increased activity of NADPH oxidase, a multisubunit membrane-bound oxidase that generates superoxide by transferring electrons from NADPH to molecular oxygen [18]. NADPH oxidases are expressed in cardiac myocytes and fibroblasts and are thought to mediate, through oxidative stress, the development and progression of LV remodeling associated with heart failure [18, 19]. Indeed, oxidative stress is increased in human heart failure and animal models of hypertrophy and fibrosis. In *ob/ob* hearts, impaired cardiac contractile performance is accompanied by elevated oxidative stress, re-expression of β-MHC and oxidative modification of SERCA2a [44]. Moreover, *ob/ob* hearts showed increased activation of NADPH oxidase and although treatment with apocynin, a NADPH oxidase inhibitor, improved the ROS-induced depression of the contractile response, it did not reverse the oxidative modification of SECRA2a [44]. It is also generally accepted that ROS can trigger apoptosis in cardiomyocytes *in vitro* and *in vivo*, possibly through a pathway involving Caspase-3 activation. Resistin-induced increase in NADPH oxidase-derived ROS in cardiomyocytes observed in our study is evidence of marked stimulation of oxidative stress. How resistin might induce ROS generation or what are the signaling mechanisms underlying this process is not currently known, primarily due to the fact that a resistin receptor has not been identified yet. Based on our results and on previous studies, it is tempting to hypothesize that the detrimental effects of resistin on cardiomyocytes can largely be explained by the chronic activation of oxidative stress pathways, that leads to a successive initiation of a detrimental program of inflammatory,

extracellular matrix remodeling, apoptosis and $Ca^{2+}$ dysregulation which could all contribute to cardiac functional impairment.

Overall, our studies demonstrate the ability of resistin, when overexpressed in the heart and in cardiomyocytes, as it is the case in diabetes, to recapitulate a molecular, pathologic and hemodynamic phenotype similar to diabetic cardiomyopathy. Resistin-induced oxidative stress may be the underlying mechanism governing cardiac remodeling in hyperresistinemia conditions.

## Acknowledgments

**Acknowledgements/Sources of Funding**

This study was supported in part by grants from the National Institutes of Health NIH/NHLBI (DL, RJH) and a Leducq Transatlantic Network through the CAERUS network (RJH). LH is supported by an NIH K01 award and ERC by an NIH Training grant.

## References

1. Steppan CM, Bailey ST, Bhat S, Brown EJ, Banerjee RR, Wright CM, et al. The hormone resistin links obesity to diabetes. Nature. 2001; 409(6818):307–12. [PubMed: 11201732]
2. Burnett MS, Lee CW, Kinnaird TD, Stabile E, Durrani S, Dullum MK, et al. The potentialrole of resistin in atherogenesis. Atherosclerosis. 2005; 182(2):241–8. [PubMed: 16159596]
3. Wang BW, Hung HF, Chang H, Kuan P, Shyu KG. Mechanical stretch enhances the expression of resistin gene in cultured cardiomyocytes via tumor necrosis factor-alpha. Am J Physiol Heart Circ Physiol. 2007; 293(4):H2305–12. [PubMed: 17573461]
4. Karakikes I, Kim M, Hadri L, Sakata S, Sun Y, Zhang W, et al. Gene remodeling in type 2 diabetic cardiomyopathy and its phenotypic rescue with SERCA2a. PloS one. 2009; 4(7):e6474. [PubMed: 19649297]
5. Gualillo O, Gonzalez-Juanatey JR, Lago F. The emerging role of adipokines as mediators of cardiovascular function: physiologic and clinical perspectives. Trends Cardiovasc Med. 2007; 17(8):275–83. [PubMed: 18021938]
6. Gao J, Chang Chua C, Chen Z, Wang H, Xu X, RCH, et al. Resistin, an adipocytokine, offers protection against acute myocardial infarction. Journal of Molecular and Cellular Cardiology. 2007; 43(5):601–9. [PubMed: 17904155]
7. Rothwell SE, Richards AM, Pemberton CJ. Resistin worsens cardiac ischaemia-reperfusion injury. Biochemical and Biophysical Research Communications. 2006; 349(1):400–7. [PubMed: 16934751]
8. Frankel DS, Vasan RS, D'Agostino RB Sr, Benjamin EJ, Levy D, Wang TJ, et al. Resistin, adiponectin, and risk of heart failure the Framingham offspring study. Journal of the American College of Cardiology. 2009; 53(9):754–62. [PubMed: 19245965]
9. Kim M, Oh JK, Sakata S, Liang I, Park W, Hajjar RJ, et al. Role of resistin in cardiac contractility and hypertrophy. Journal of Molecular and Cellular Cardiology. 2008; 45(2):270–80. [PubMed: 18597775]
10. Suckau L, Fechner H, Chemaly E, Krohn S, Hadri L, Kockskamper J, et al. Long-term cardiac-targeted RNA interference for the treatment of heart failure restores cardiac function and reduces pathological hypertrophy. Circulation. 2009; 119(9):1241–52. [PubMed: 19237664]
11. Lang RM, Bierig M, Devereux RB, Flachskampf FA, Foster E, Pellikka PA, et al. Recommendations for chamber quantification: a report from the American Society of Echocardiography's Guidelines and Standards Committee and the Chamber Quantification Writing Group, developed in conjunction with the European Association of Echocardiography, a branch of the European Society of Cardiology. J Am Soc Echocardiogr. 2005; 18(12):1440–63. [PubMed: 16376782]
12. Gueret P, Meerbaum S, Zwehl W, Wyatt HL, Davidson RM, Uchiyama T, et al. Two-dimensional echocardiographic assessment of left ventricular stroke volume: experimental correlation with

thermodilution and cineangiography in normal and ischemic states. Cathet Cardiovasc Diagn. 1981; 7(3):247–58. [PubMed: 7285103]

13. Pacher P, Nagayama T, Mukhopadhyay P, Batkai S, Kass DA. Measurement of cardiac function using pressure-volume conductance catheter technique in mice and rats. Nat Protoc. 2008; 3(9): 1422–34. [PubMed: 18772869]
14. Saha JK, Xia J, Grondin JM, Engle SK, Jakubowski JA. Acute hyperglycemia induced by ketamine/xylazine anesthesia in rats: mechanisms and implications for preclinical models. Exp Biol Med. 2005; 230(10):777–84.
15. Sato N, Kobayashi K, Inoguchi T, Sonoda N, Imamura M, Sekiguchi N, et al. Adenovirus-mediated high expression of resistin causes dyslipidemia in mice. Endocrinology. 2005; 146(1): 273–9. [PubMed: 15471967]
16. Satoh H, Nguyen MT, Miles PD, Imamura T, Usui I, Olefsky JM. Adenovirus-mediated chronic "hyper-resistinemia" leads to in vivo insulin resistance in normal rats. The Journal of Clinical Investigation. 2004; 114(2):224–31. [PubMed: 15254589]
17. Vandecaetsbeek I, Raeymaekers L, Wuytack F, Vangheluwe P. Factors controlling the activity of the SERCA2a pump in the normal and failing heart. Biofactors. 2009; 35(6):484–99. [PubMed: 19904717]
18. Maejima Y, Kuroda J, Matsushima S, Ago T, Sadoshima J. Regulation of myocardial growth and death by NADPH oxidase. Journal of Molecular and Cellular Cardiology. 2011; 50(3):408–16. [PubMed: 21215757]
19. Sawyer DB, Siwik DA, Xiao L, Pimentel DR, Singh K, Colucci WS. Role of oxidative stress in myocardial hypertrophy and failure. Journal of Molecular and Cellular Cardiology. 2002; 34(4): 379–88. [PubMed: 11991728]
20. Murdoch CE, Zhang M, Cave AC, Shah AM. NADPH oxidase-dependent redox signalling in cardiac hypertrophy, remodelling and failure. Cardiovascular Research. 2006; 71(2):208–15. [PubMed: 16631149]
21. Byrne JA, Grieve DJ, Bendall JK, Li JM, Gove C, Lambeth JD, et al. Contrasting roles of NADPH oxidase isoforms in pressure-overload versus angiotensin II-induced cardiac hypertrophy. Circulation Research. 2003; 93(9):802–5. [PubMed: 14551238]
22. Heymes C, Bendall JK, Ratajczak P, Cave AC, Samuel JL, Hasenfuss G, et al. Increased myocardial NADPH oxidase activity in human heart failure. Journal of the American College of Cardiology. 2003; 41(12):2164–71. [PubMed: 12821241]
23. Bokarewa M, Nagaev I, Dahlberg L, Smith U, Tarkowski A. Resistin, an adipokine with potent proinflammatory properties. J Immunol. 2005; 174(9):5789–95. [PubMed: 15843582]
24. Nagaev I, Bokarewa M, Tarkowski A, Smith U. Human resistin is a systemic immune-derived proinflammatory cytokine targeting both leukocytes and adipocytes. PloS one. 2006; 1:e31. [PubMed: 17183659]
25. Silswal N, Singh AK, Aruna B, Mukhopadhyay S, Ghosh S, Ehtesham NZ. Human resistin stimulates the pro-inflammatory cytokines TNF-alpha and IL-12 in macrophages by NF-kappaB-dependent pathway. Biochemical and Biophysical Research Communications. 2005; 334(4):1092–101. [PubMed: 16039994]
26. Cucoranu I, Clempus R, Dikalova A, Phelan PJ, Ariyan S, Dikalov S, et al. NAD(P)H oxidase 4 mediates transforming growth factor-beta1-induced differentiation of cardiac fibroblasts into myofibroblasts. Circulation research. 2005; 97(9):900–7. [PubMed: 16179589]
27. Siwik DA, Pagano PJ, Colucci WS. Oxidative stress regulates collagen synthesis and matrix metalloproteinase activity in cardiac fibroblasts. American Journal of Physiology. 2001; 280(1):C53–60. [PubMed: 11121376]
28. Dobrin JS, Lebeche D. Diabetic cardiomyopathy: signaling defects and therapeutic approaches. Expert Review of Cardiovascular Therapy. 2010; 8(3):373–91. [PubMed: 20222816]
29. Harmancey R, Taegtmeyer H. The complexities of diabetic cardiomyopathy: lessons from patients and animal models. Curr Diab Rep. 2008; 8(3):243–8. [PubMed: 18625124]
30. Hayata N, Fujio Y, Yamamoto Y, Iwakura T, Obana M, Takai M, et al. Connective tissue growth factor induces cardiac hypertrophy through Akt signaling. Biochemical and Biophysical Research Communications. 2008; 370(2):274–8. [PubMed: 18375200]

31. Panek AN, Posch MG, Alenina N, Ghadge SK, Erdmann B, Popova E, et al. Connective tissue growth factor overexpression in cardiomyocytes promotes cardiac hypertrophy and protection against pressure overload. PloS one. 2009; 4(8):e6743. [PubMed: 19707545]
32. Aragno M, Mastrocola R, Medana C, Catalano MG, Vercellinatto I, Danni O, et al. Oxidative stress-dependent impairment of cardiac-specific transcription factors in experimental diabetes. Endocrinology. 2006; 147(12):5967–74. [PubMed: 16935841]
33. Yoon PO, Lee MA, Cha H, Jeong MH, Kim J, Jang SP, et al. The opposing effects of CCN2 and CCN5 on the development of cardiac hypertrophy and fibrosis. Journal of Molecular and Cellular Cardiology. 2010; 49(2):294–303. [PubMed: 20430035]
34. Westermann D, Van Linthout S, Dhayat S, Dhayat N, Schmidt A, Noutsias M, et al. Tumor necrosis factor-alpha antagonism protects from myocardial inflammation and fibrosis in experimental diabetic cardiomyopathy. Basic Res Cardiol. 2007; 102(6):500–7. [PubMed: 17909696]
35. Ares-Carrasco S, Picatoste B, Benito-Martin A, Zubiri I, Sanz AB, Sanchez-Nino MD, et al. Myocardial fibrosis and apoptosis, but not inflammation, are present in long-term experimental diabetes. Am J Physiol Heart Circ Physiol. 2009; 297(6):H2109–19. [PubMed: 19820199]
36. Choi KM, Zhong Y, Hoit BD, Grupp IL, Hahn H, Dilly KW, et al. Defective intracellular Ca(2+) signaling contributes to cardiomyopathy in Type 1 diabetic rats. Am J Physiol Heart Circ Physiol. 2002; 283(4):H1398–408. [PubMed: 12234790]
37. Vafiadaki E, Arvanitis DA, Pagakis SN, Papalouka V, Sanoudou D, Kontrogianni-Konstantopoulos A, et al. The anti-apoptotic protein HAX-1 interacts with SERCA2 and regulates its protein levels to promote cell survival. Mol Biol Cell. 2009; 20(1):306–18. [PubMed: 18971376]
38. Vafiadaki E, Sanoudou D, Arvanitis DA, Catino DH, Kranias EG, Kontrogianni-Konstantopoulos A. Phospholamban interacts with HAX-1, a mitochondrial protein with anti-apoptotic function. J Mol Biol. 2007; 367(1):65–79. [PubMed: 17241641]
39. Pinton P, Giorgi C, Siviero R, Zecchini E, Rizzuto R. Calcium and apoptosis: ER-mitochondria Ca2+ transfer in the control of apoptosis. Oncogene. 2008; 27(50):6407–18. [PubMed: 18955969]
40. Lee Y, Gustafsson AB. Role of apoptosis in cardiovascular disease. Apoptosis. 2009; 14(4):536–48. [PubMed: 19142731]
41. Chen C, Jiang J, Lu JM, Chai H, Wang X, Lin PH, et al. Resistin decreases expression of endothelial nitric oxide synthase through oxidative stress in human coronary artery endothelial cells. Am J Physiol Heart Circ Physiol. 2010; 299(1):H193–201. [PubMed: 20435848]
42. Verma S, Li SH, Wang CH, Fedak PW, Li RK, Weisel RD, et al. Resistin promotes endothelial cell activation: further evidence of adipokine-endothelial interaction. Circulation. 2003; 108(6): 736–40. [PubMed: 12874180]
43. Umar S, van der Laarse A. Nitric oxide and nitric oxide synthase isoforms in the normal, hypertrophic, and failing heart. Mol Cell Biochem. 2010; 333(1–2):191–201. [PubMed: 19618122]
44. Li SY, Yang X, Ceylan-Isik AF, Du M, Sreejayan N, Ren J. Cardiac contractile dysfunction in Lep/Lep obesity is accompanied by NADPH oxidase activation, oxidative modification of sarco(endo)plasmic reticulum Ca2+-ATPase and myosin heavy chain isozyme switch. Diabetologia. 2006; 49(6):1434–46. [PubMed: 16612592]

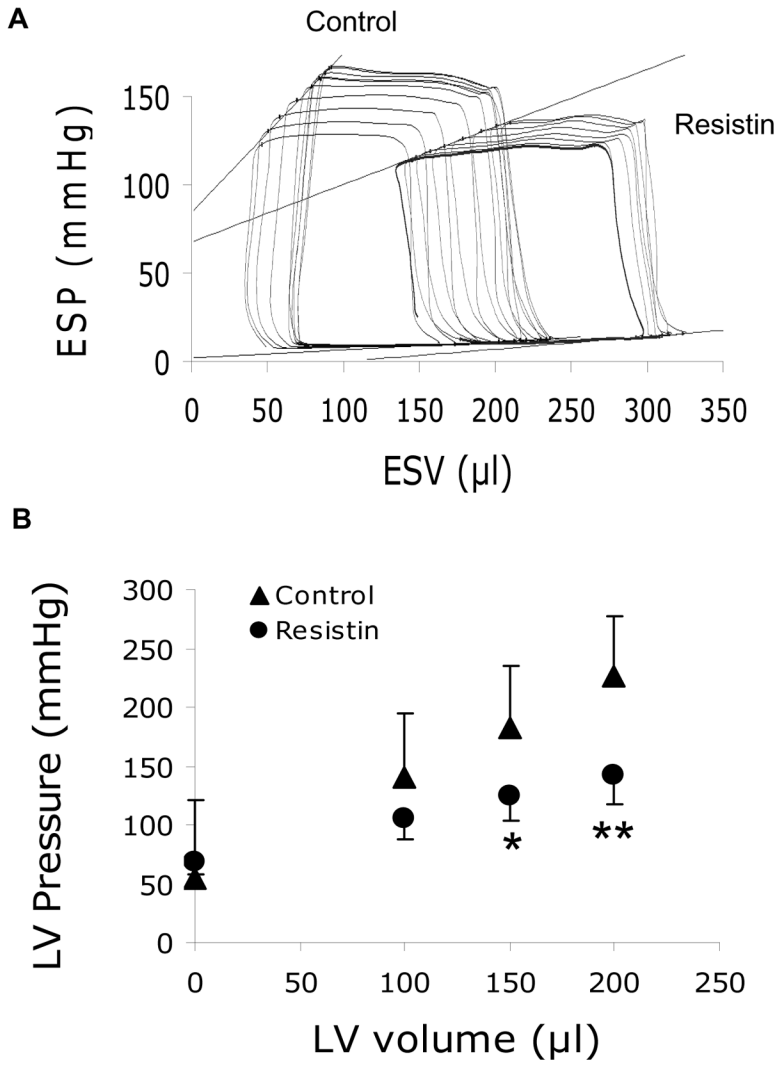


**Figure 1. Reduced load-independent LV contractility associated with resistin overexpression**

(A), Representative end-systolic pressure volume relationship (ESPVR) tracings for control and AAV9-resistin injected-groups. (B), Comparative pressures at equal volumes in both groups based on ESPVR equation. **P*<0.05, ***P*<0.01.

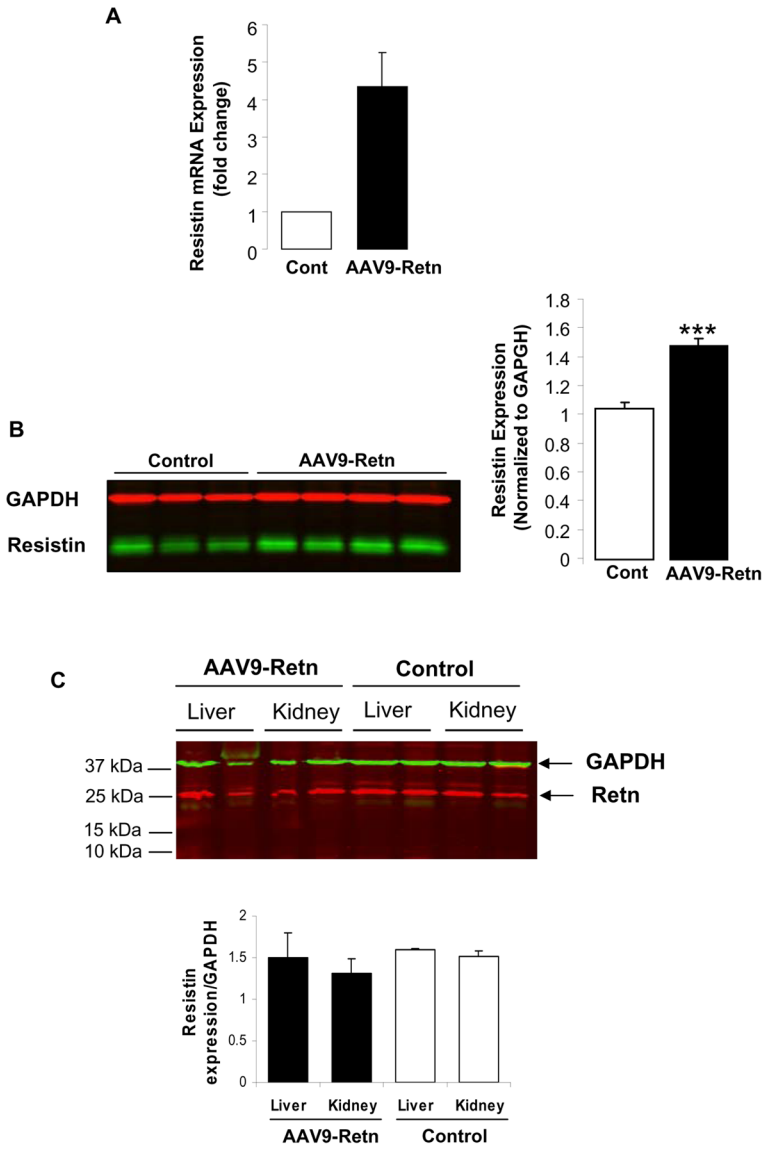


**Figure 2. Upregulation of resistin mRNA and protein levels in heart tissue of AAV9-Retn injected-animals**

(A), qRT-PCR of resistin expression in LV tissues from control and AAV9-Retn-treated animals. (B), a representative Western-blot analysis of resistin protein level in LV tissue with histograms showing relative resistin expression normalized to GAPDH. (C), a representative Western-blot analysis and quantification of resistin protein levels in liver and kidney tissues from control and AAV9-Retn-treated animals. Data shown are mean ± SD (***$P$<0.001 vs. control animals).

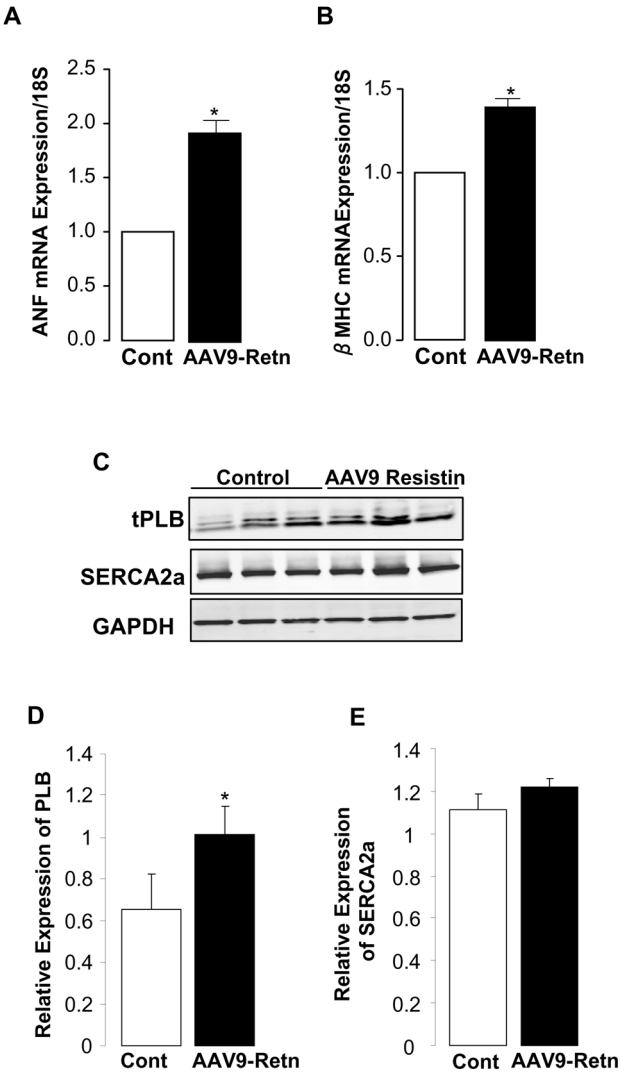


**Figure 3. Expression of hypertrophy markers and calcium regulatory proteins**

Quantitative real-time PCR of ANF (A) and β-MHC (B) mRNA in LV tissue overexpressing resistin using primers specific to rat genes. Fold changes in gene expression in resistin-overexpressing animals versus controls were determined using the ΔΔCt method with normalization to 18S. A representative Western-blot analysis of phospholamban (PLB) and SERCA2a proteins levels in LV tissue from control and AAV9-Retn-treated hearts (C) with histograms showing relative PLB (D) and SERCA2a (E) expression normalized to GAPDH. Data shown are mean ± SD, **P*<0.05.

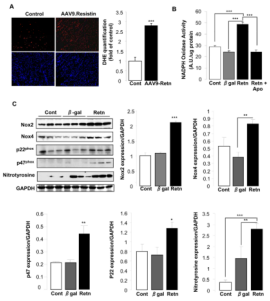

**Figure 4. Resistin induces oxidative stress in cardiomyocytes**

(A), DHE fluorescence staining for superoxide in LV tissue sections from control and AAV9-Retn-treated animals with quantification of DHE staining. (B), NADPH oxidase activity measured by lucigenin-enhanced chemiluminescence in cardiomyocytes without or with Apocynin (Retn + Apo), an inhibitor of NADPH oxidase. (C), representative Western blots for Nox2, Nox4, $p22^{phox}$, $p47^{phox}$, and nitrotyrosine and their respective quantification in control (Cont) non-infected cardiomyocytes or cardiomyocytes infected with β-gal or Retn adenoviruses. Data shown are mean ± SD, ***P*<0.01; ****P*<0.001.

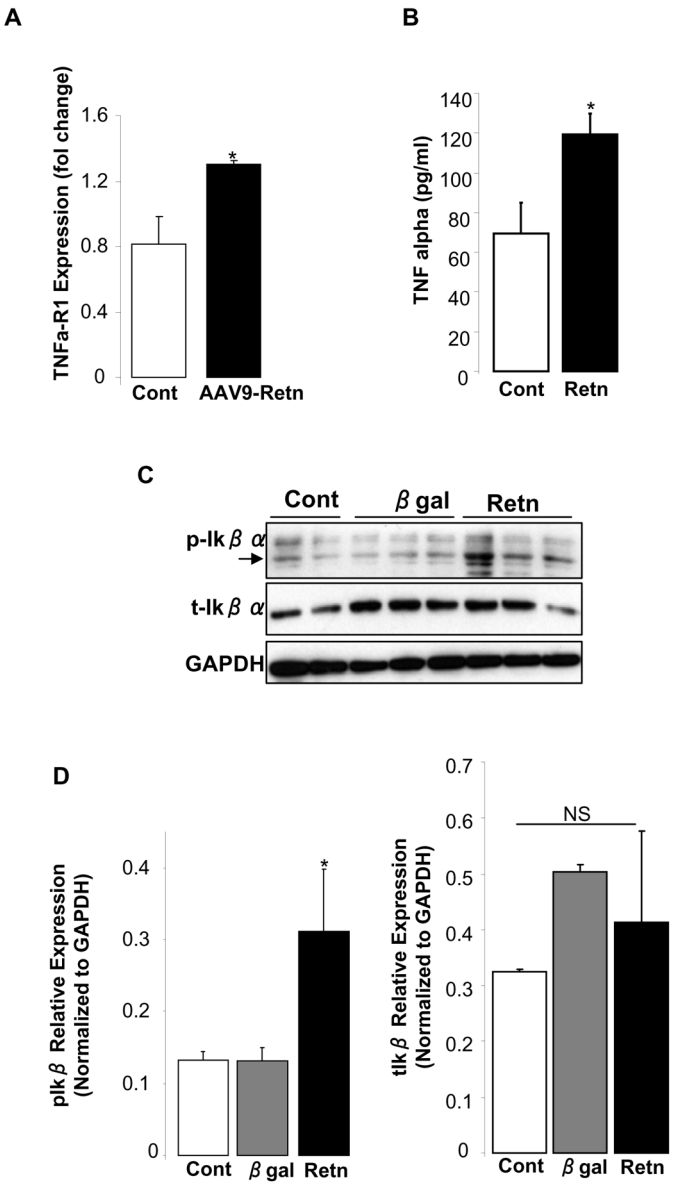


**Figure 5. Resistin overexpression induces pro-inflammatory proteins *in vivo* and *in vitro***

(A), Quantitative real-time PCR of TNFα-R1 mRNA levels in LV tissue-overexpressing resistin relative to controls. Fold changes in gene expression were determined using the ΔΔCt method with normalization to 18S. (B), Adult rat cardiomyocytes infected with adenovirus encoding resistin release more TNFα into the media compared to controls. (C), Representative Western-blot analysis of phospho- IκBα and total IκBα protein expression in control uninfected adult rat cardiomyocytes or myocytes overexpressing resistin (Retn), or beta-galactosidase (β-gal). (D), Histogram showing relative phospho- IκBα and total IκBα protein expression normalized to GAPDH. Data shown are mean ± SD from three independent experiments. $*P < 0.05$.

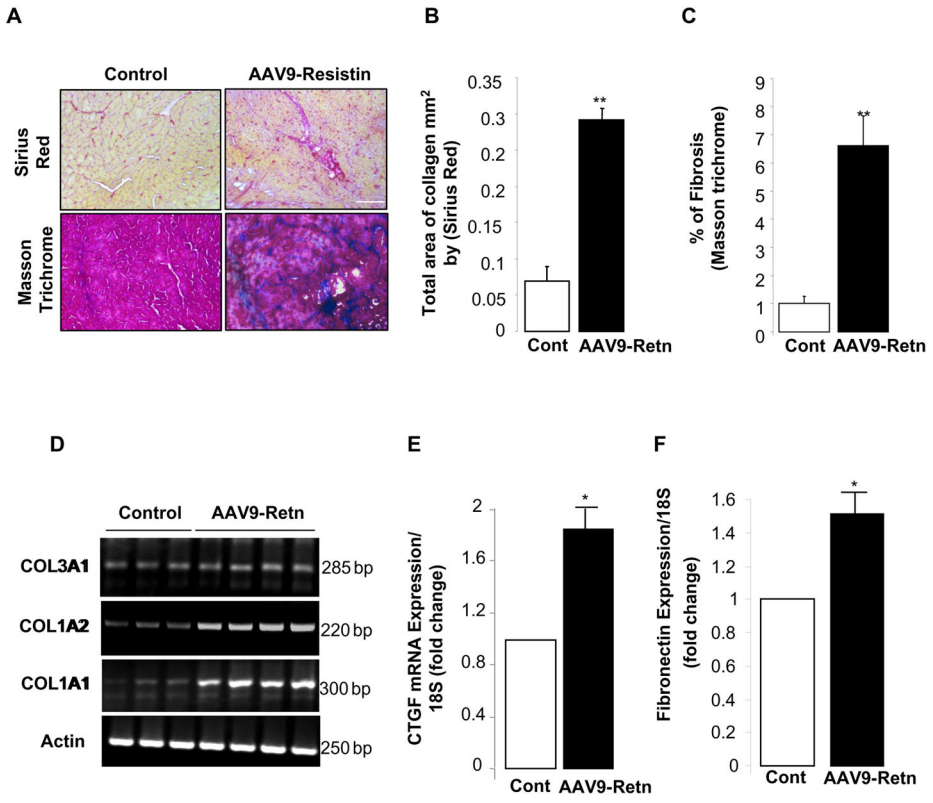


**Figure 6. Long-term overexpression of resistin induces myocardial fibrosis**

(A), Sirius Red and Masson Trichrome staining of LV tissue from control and AAV9-Retn injected-animals. Fibrosis quantification of total area of collagen per $mm^2$ by Sirius Red (B) and cardiac fibrosis quantification as percentage of blue stained area (fibrotic) vs. control using Masson Trichrome (C). mRNA levels of collagen subtypes types 1 and 3 (D), connective tissue growth factor (CTGF) (E), and fibronectin (F) by relative quantification compared to controls. Data shown are from at least three independent determinations. **P*<0.05, ***P*<0.01.

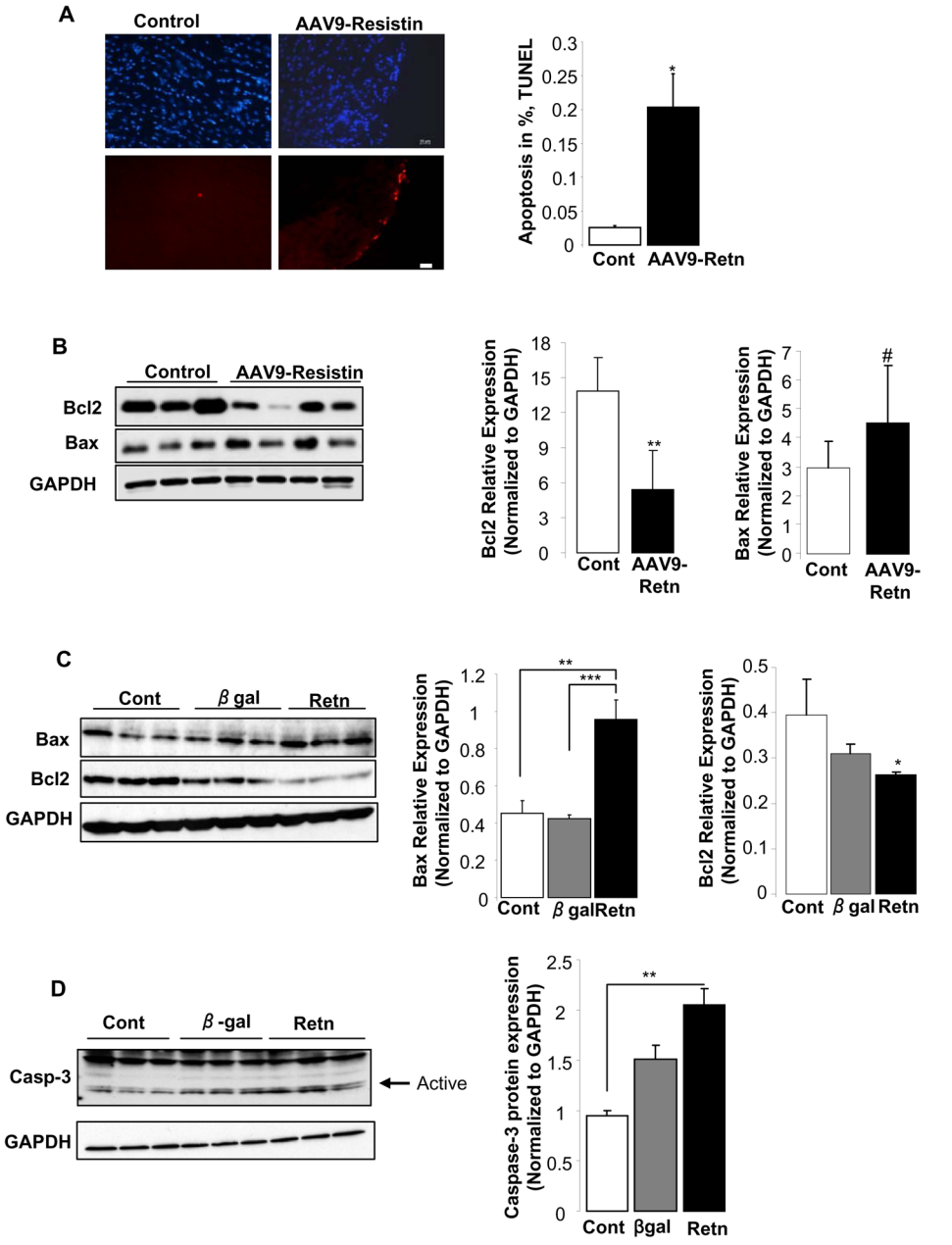


**Figure 7. Resistin overexpression induces cardiac apoptosis**

(A), TUNEL staining of apoptotic cells in resistin-overexpressing and control LV tissues. Bar = 10μm and quantification of apoptosis shown as a percentage of apoptotic nuclei (red by TUNEL) vs. total nuclei (blue by DAPI). (B), Western-blot analysis of pro-apoptotic Bax and anti-apoptotic Bcl-2 protein levels in LV tissue from animals overexpressing resistin and control animals with histograms showing normalized expression of Bax and Bcl2 to GAPDH. (C), Bax and Bcl-2 protein expression *in vitro* in cardiomyocytes overexpressing resistin or β-gal, and in control non-infected cells with histograms showing normalized expression to GAPDH. (D), Western blot showing active Caspase-3 protein levels in cardiomyocytes overexpressing resistin or β-gal and in control non-infected myocytes with histogram showing normalized expression of Caspase-3 to GAPDH. Data shown are mean ± SD from at least three independent experiments. $^{\#}P$=0.05, * $P$<0.05, ** $P$<0.01, *** $P$<0.001.

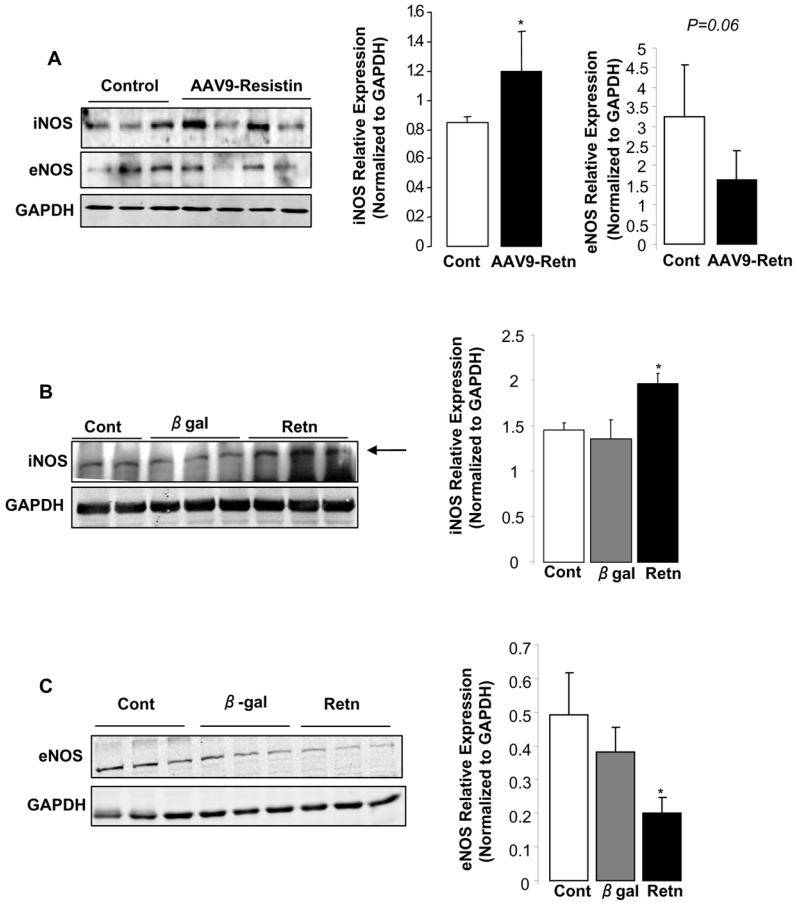


**Figure 8. Effect of resistin on the expression of iNOS and eNOS**

A, Representative Western blot analysis of iNOS and eNOS protein expression in resistin overexpressing LV tissue *in vivo*, with histogram showing relative iNOS and eNOS ratios normalized to GAPDH. Western blot analysis of iNOS (B) and eNOS (C) protein expression in cardiomyocytes overexpressing resistin or β-gal and in control non-infected cells with histogram showing relative iNOS (B) and eNOS (C) ratios normalized to GAPDH. Data shown are mean ± SD from at least three independent experiments. **P*<0.05.

**Table 1**

Morphometric and echocardiographic analyses (mean±SD).

| Group | Control (n=8) | Resistin (n=5) |
|---|---|---|
| **Morphometric analysis** | | |
| Body Weight (g) | 625±25 | 553±42(*) |
| LV weight (g) | 1.03±0.09 | 1.04±0.07 |
| Right ventricular weight (g) | 0.27±0.04 | 0.23±0.02 |
| LV weight/Body Weight (mg/g) | 1.64±0.10 | 1.88±0.13(*) |
| Right ventricular weight/Body Weight (mg/g) | 0.44±0.04 | 0.43±0.06 |
| **M-mode echocardiography** | | |
| Heart Rate (beats/minute) | 401±34 | 410±27 |
| Anteroseptal LV wall thickness in diastole (mm) | 2.2±0.2 | 2.1±0.2 |
| Posterior LV wall thickness in diastole (mm) | 2.3±0.2 | 2.4±0.2 |
| LV diastolic internal diameter (mm) | 6.6±0.4 | 7.1±0.5(*) |
| LV systolic internal diameter (cm) | 2.7±0.2 | 3.2±0.8 |
| LV fractional shortening (%) | 59.8±3.1 | 54.5±9.8 |
| Aortic diameter (mm) | 3.6±0.3 | 3.8±0.4 |
| Left atrial diameter (mm) | 2.9±0.5 | 3.4±0.6 |
| **2D echocardiography** | | |
| LV end-diastolic volume, by area-length (ml) | 0.39±0.08 | 0.47±0.09 |
| LV end-systolic volume, by area-length (ml) | 0.06±0.02 | 0.10±0.03(*) |
| LV ejection fraction, by area-length (%) | 84.7±4.1 | 77.7±8.3 |

LV, left ventricle;

*$P<0.05$ vs. control.

## Table 2

Left ventricular invasive hemodynamics by pressure-volume conductance catheters (mean±SD).

| Group | Control (n=6) mean±SD | Resistin (n=5) mean±SD |
|---|---|---|
| **Steady state hemodynamics** | | |
| Heart Rate (beats/minute) | 343 ± 21 | 349 ± 12 |
| Pmax (mmHg) | 136 ± 18 | 119 ± 14 |
| LV-end-diastolic pressure (mmHg) | 6 ± 2 | 7 ± 2 |
| dP/dt max (mmHg/s) | 8460 ± 725 | 8843 ± 1321 |
| dP/dt min (mmHg/s) | −7319 ± 924 | −6809 ± 1287 |
| **Hemodynamics with inferior vena cava occlusion** | | |
| ESPVR slope (mmHg/μl) | 0.86 ± 0.24 | 0.37 ± 0.08** |
| EDPVR slope (mmHg/μl) | 0.05 ± 0.01 | 0.05 ± 0.02 |
| Vo ESPVR (μl) | −80 ± 96 | −184 ± 11* |
| Volume intercept EDPVR (μl) | 56 ± 99 | 66 ± 80 |

LV, left ventricle; Pmax, maximal pressure of the LV; ESPVR, end-systolic pressure volume relationship; EDPVR end-diastolic pressure-volume relationship. Vo ESPVR and volume intercept EDPVR represent volumes when pressure is zero according to the ESPVR and EDPVR lines intersecting with the volume axis (see figure 1);

* $P<0.05$;

** $P<0.01$.